

Biomechanical properties of the thin PVD coatings defined by red blood cells

K. TREMBECKA-WOJCIGA¹, R. MAJOR^{1*}, J.M. LACKNER², F. BRUCKERT³,
E. JASEK⁴, and B. MAJOR¹

¹ Institute of Metallurgy and Materials Science; Polish Academy of Sciences, 25 Reymonta St., 30-059 Cracow, Poland

² Joanneum Research Forschungsges mbH, Institute of Surface Technologies and Photonics, Functional Surfaces,
Leobner Strasse 94, A-8712 Niklasdorf, Austria

³ Laboratoire des Matériaux et du Génie Physique, Grenoble Institute of Technology – Minatec,
3 Parvis Louis Néel, BP 257, 38016 Grenoble Cedex 1, France

⁴ Department of Histology, Jagiellonian University Medical College, 7 Kopernika St., 31-034 Cracow, Poland

Abstract. The measurement of the strength of bonds between biomaterials and cells is a major challenge in biotribology since it allows for the identification of different species in adhesion phenomena. Biomaterials, such as diamond-like carbon (DLC), titanium, and titanium nitride, seem to be good candidates for future blood-contact applications. These materials were deposited as thin films by the hybrid pulsed laser deposition (PLD) technique to examine the influence of such surfaces on cell behavior. The biomaterial examinations were performed in static conditions with red blood cells and then subjected to a dynamical test to observe the cell detachment kinetics. The tests revealed differences in behavior with respect to the applied coating material. The strongest cell-biomaterial interaction was observed for the carbon-based materials compared to the titanium and titanium nitride. Among many tests, a radial flow interaction analysis gives the opportunity to analyze cell adhesion to the applied material with the high accuracy. Analysis of concentrates helped to select materials for further dynamic tests on blood using an aortic flow simulator. In this case, the platelet adhesion to the surface and their degree of activation was analyzed. The quality of the selected coating was tested using a scratch test. The analyses of the microstructure were done using high resolution transmission electron microscopy. The phase composition and the residual stress were analyzed using X-ray diffraction methods.

Key words: biomechanical properties, thin PVD coatings, red blood cells.

1. Introduction

Analysis of blood-material interaction is a challenge for scientists due to both incomplete understanding of biological pathways to material failure and the designers' inability to fully evaluate blood material failure and blood material responses. In the development of materials with lower thrombogenicity, researchers have primarily focused their efforts on modifying surfaces. This approach is reasonable, since it is only the surface chemistry of a material that should dictate its biological responses and the mechanical characteristics of the material are primarily dictated by the bulk chemistry. Despite successes in reducing protein and cellular deposits on some materials, a truly non-thrombogenic surface does not exist.

For the last twenty years, experimental and theoretical works have been dedicated to cell adhesion from three very different perspectives [1]. From the biological point of view, understanding of the molecular mechanisms is of central importance, i.e., understanding when a cell adheres, rolls, or slides on passive or reactive substrates. Many functions performed by living cells depend on these properties. From a physico-chemical point of view, bioadhesion involves cells, a solid substrate, and a liquid medium [1]. The relevant properties of a microorganism are the hydrophobicity and charge of the cell surface, cell size, and possession. A lot of ex-

perimental and theoretical works have been dedicated to cell adhesion [2]. From the physical point of view, even the passive (non-reactive) response of cells to an external force offers new phenomena that find no equivalent in more traditional materials. This is the case in bioadhesion phenomena, where the discrete nature of contact regions, the weak or non-covalent bonding of the cell to the substrate, and the multi-component variety of the cytoplasmic membrane or of its extracellular matrix are the origin of contact forces. Measuring the strength of these bonds is a major challenge in cellular biology since it allows for the identification of the different factors at work in adhesion phenomena. Creation of new types of biomaterials requires evaluation of reactions occurring during their contact with tissue. Testing the blood-material interaction of biomedical materials aims to detect adverse interaction between artificial surface and blood elements. International Organization for Standardization (ISO) developed a guidance on testing medical materials that have contact with blood elements (ISO 10933-4). According to this norm, haemocompatible material must not adversely interact with any blood components [1–5].

The blood-biomaterial contact is followed by a rapid plasma protein adsorption, which leads to the activation of the coagulation system. In addition, the surface contact or rate forces can cause a damage of the red blood cell membrane, which results in hemolysis. These surface interactions occur

*e-mail:r.major@imim.pl

at the artificial materials as well as at the blood elements. Because of this, the cells damage, which is induced by the test setup, should be well defined [6].

In recent years, testing systems have been established. Commonly used test conditions mimicking vascular flow aim to simulate dynamic interaction between whole blood and bio-material [7, 8]. A dynamic test differs from a static interaction by shear forces activating blood cells. The parallel-plate flow chamber system was widely used to investigate the adhesion of cells in flow conditions [9, 10].

The aim of this work is to describe the tribological and biotribological interaction. The biotribological analysis concerns detachment kinetics of red blood cells, which would simulate some aspects of the behavior of blood cells in dynamic conditions when they are in contact with different biocompatible materials. These materials were deposited as thin films, allowing only the surface to be modified and not the bulk of the material. The cell material was analyzed and the attempts of explaining the measurements were undertaken in terms of surface engineering and finite element modeling. The following coatings were taken under the consideration a-C:H:Si, SiO₂, TiO_x and a-C:H. Thin coatings were deposited using magnetron sputtering technique.

2. Materials and methods

2.1. Preparation of the surfaces. The development of surface modification by means of thin film materials was performed by magnetron sputtering in direct current (DC), unbalanced mode. For the work the following thin coatings were prepared: a-C:H:Si 500 nm thick, a-C:H:Si 200 nm thick, a-C:H:Si 15 nm thick, SiO₂ 15 nm thick, a-C:H 15 nm thick, TiO_x 15 nm. Titanium (medical grade titanium for titanium and titanium nitride coatings) and carbon targets (the latter for Diamond Like Carbon-DLC) were used to deposit films on silicon wafer substrates at room temperature in an argon atmosphere (diamond-like carbon (DLC) and titanium (Ti)) or nitrogen-argon atmosphere (for nitrides). To ensure homogenous film thickness over the entire coated surfaces, substrates were rotated during deposition at a speed of 5.4 cm s⁻¹ through the plasma plumes. A detailed description of the deposition arrangement is given elsewhere [11].

2.2. Analysis of the mechanical properties of the coatings. Mechanical properties evaluation of the materials prepared de novo for the biomedical application is important. Biocompatibility strongly depends on the mechanical properties. In order to determine mechanical adhesion of the thin layer to the substrate, the indentation tests and the scratch tests were done.

The indentation tests considered the Rockwell indenter of the tip radius of 20 μm. The analysis are based on indentation of hardness of a material [12].

The tests were performed at two loads, 200 and 1000 mN. The maximum penetration depth at these loads was respectively 55 and 120 μm, that means the depth was many times larger than the thickness of coatings.

A scratch test was applied in order to characterize the mechanical properties of thin films, e.g. adhesion, fracture and deformation. The scratch test allow to characterize the film-substrate system and to quantify parameters such as friction and adhesive strength. In the thin film diagnosis it is an invaluable tool for research, development and quality control. The scratch test was carried out using the standard Rockwell indenter with the tip of 0.2 mm. The load range was 0–20 N towards scratching distance equal to 5 mm.

2.3. Protein-material interactions. Protein interaction with material surfaces is an important and complex problem, with many biological, medical and pharmaceutical applications. These interactions involve protein conformational changes, coupled to a reorganization of material surfaces. The protein-material interaction test was related to the analysis of protein adsorption on the tested surfaces. For the protein-material analysis fetal bovine serum (FBS) and human blood (blood group was B Rh+) were used. 10 times FBS dilution and 1000 times blood dilution were used in the study. There were prepared two sets of materials. The samples 1 cm² each were cleaned and put in the multiwall plate. 2–5 mL diluted FBS was poured on the top of the analyzed surface. The same volumes of blood solution were used for a second set of materials. Samples were incubated for about 12h in 37°C and mixed. Protein from the surface was removed with 0.2% sodium dodecyl sulfate solution (SDS). The results were normalized to bovine serum albumin (BSA). Proteins were analyzed with fluorescence using quantification solution- Quant-iT Protein Assay Kit purchased in Invitrogen by using Microplate Fluorescence Reader FL600 (Bio-Tek Instruments).

2.4. Analysis of the biomechanical properties of the coatings. The biomechanical properties evaluation was based on the analysis consisting of cell-material interaction in the dynamic conditions. The experiment was carried out theoretically using the finite element method and verified experimentally using a radial flow chamber.

Cell-material interaction under hydrodynamic conditions: finite element simulation. The cell-material interaction should not be regarded as a flat surface, but as a system of discrete adhesive bridges. The main premise of this model was to analyze the influence of stress on the cells examined in different places in the radial flow chamber. The finite element modeling applied to the process of cell-material interaction assumed certain simplifications that were required for numerical analysis. Cells were regarded as firmly adhesive objects in an elastic mode. The flow of the medium near a cell was calculated on the basis of the assumption taken from the real experiment: the dynamic viscosity of the fluid, $\eta = 1$ Pa·s, and the distance between disk and plate, $e = 150$ μm.

Cell-material interaction under hydrodynamic conditions: radial detachment test. A radial flow chamber was used to determine the efficiency and kinetics of model cells as a function of applied shear stress. The layout of the test is illustrated in Fig. 1. The details are described in [5–7]. The red blood cell concentrate was diluted 4000x by using a phos-

Biomechanical properties of the thin PVD coatings defined by red blood cells

phate buffered saline (PBS) (pH 7.4). The density of the red blood cells was measured by Neubauer chamber. The radial flow chamber consists of a two parallel plates with spacing between them (Fig. 2). Analyzed material of the disc-shaped was put besides two plates. Blood solution was uniformly applied to the surface of the tested materials and left for a few minutes in order to erythrocyte's adhesion to the surface (Fig. 2a,b). The distance between the disks was determined to 150 μm by using a three micrometer screws (Fig. 2c). For every coating this time was determined experimentally. After that a constant volumetric flow of PBS was pumped through the center of the upper disc and flows radially to the disc edges (Fig. 2d). A radial hydrodynamic flow is generated between the examined plate and the working disk placed above the investigated surface (Fig. 2). The flow is set by the gravity and the flow rate is defined by the difference in the height between the upstream reservoir and the pump. The flow rate is constant during the entire experiment and depends individually on the tested material. The highest applied shear stresses were not in the center of the disc but near behind a flow hole. The values of shear stress were decreasing along the radius of the disc like $1/\text{radius}$.

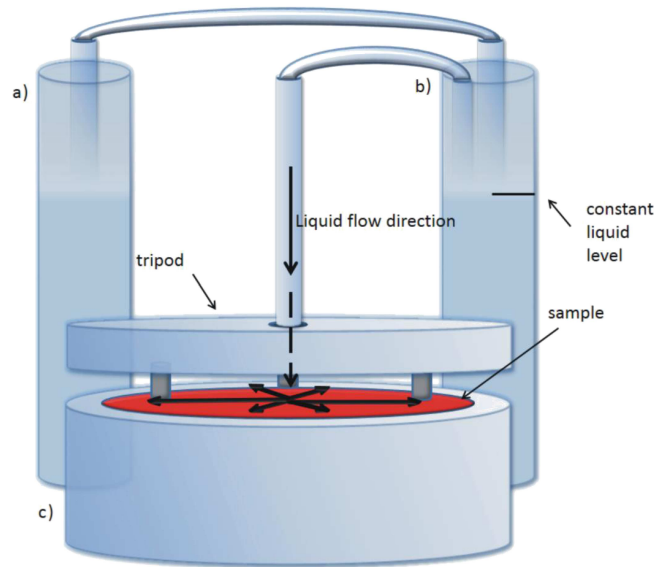


Fig. 1. Radial flow chamber assembly: a) working reservoir, b) stress determining reservoir, c) radial flow chamber

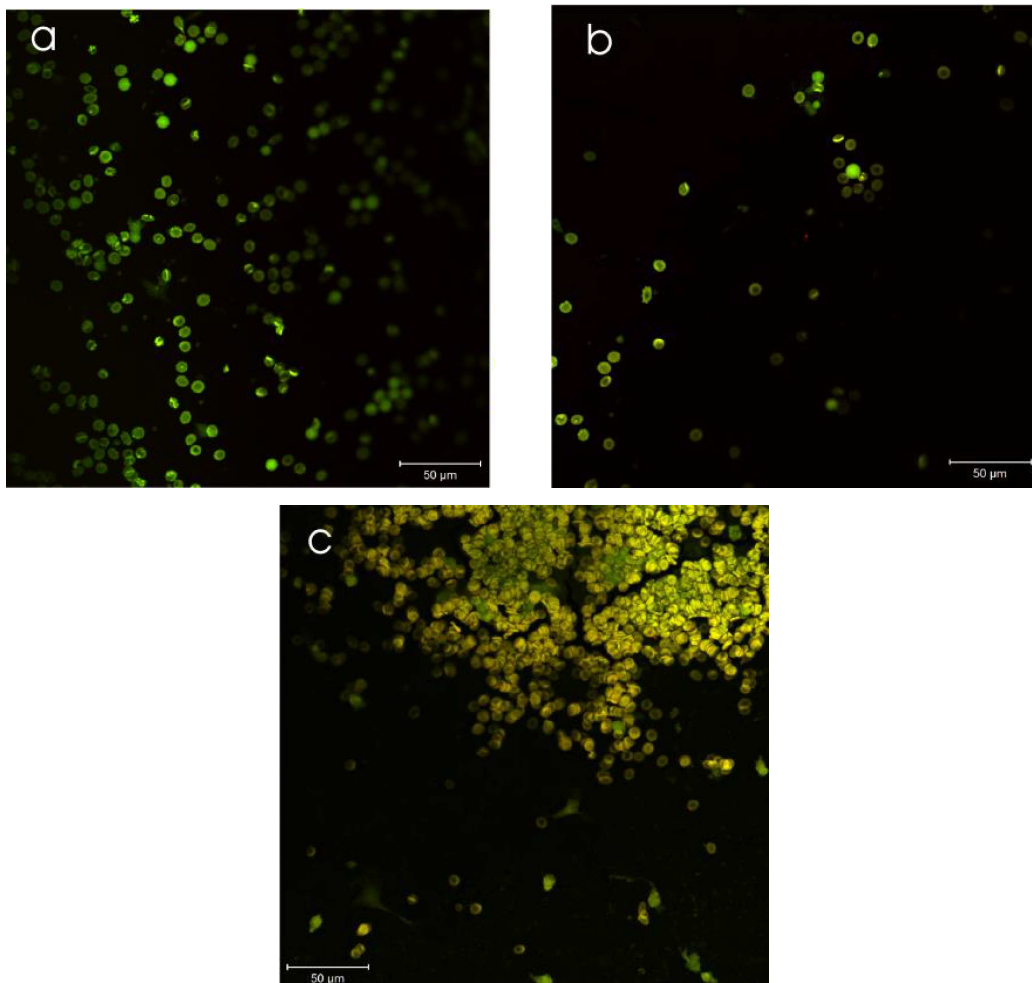


Fig. 2. Distribution of cells after the radial flow experiment: a) the stagnation point, b) highest cell washout, c) lowest cell washout

After a specified time, the experiment was stopped and the plate was transported to the microscope to be observed in a Petri dish filled with a phosphate buffered saline to keep the cells submerged. The cell distribution was recorded 150 mm to the right and left of the stagnation point. An example of the cell distribution after the radial flow experiment is presented in Fig. 3a. Stagnation point is visible in the center (Fig. 3b). Red blood cells were not removed from this location due to the rectangular impact of the flow force. The empty region, visible as a ring, corresponds to the highest shear stress zone (Fig. 3c).

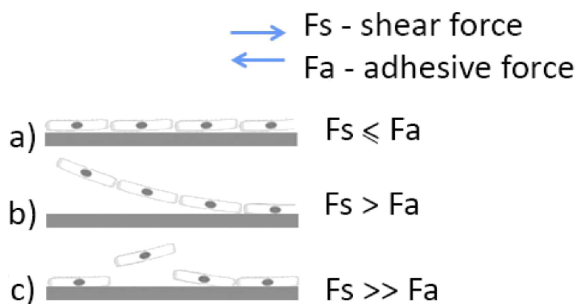


Fig. 3. Models of detachment of cells from the substrate: a) lack of detachment, b) one by one detachment, c) selective detachment

The radial flow exposition time was determined individually for the examined material. In most cases, 100% of the remaining cells were at a distance of 4 mm from the center after the completion of the shear flow test.

Cell detachment. For a given cell, detachment occurs above a threshold of the applied hydrodynamic stress. This threshold stress depends on cell size and the physico-chemical properties of the applied substrate. In contrast, the kinetics of cell detachment is almost independent of cell size and is strongly affected by substrate modification.

Depending on the value of the applied stress, there are three models of detached cell behavior described by Demilly et al. [13] (Fig. 4). In the first model, where the values of applied shear forces are less or equal to the values of adhesive forces, cells are not detached from the surface (Fig. 4a). When shear forces have bigger values than adhesive there can be observed two models of detachment. In the first one, where this difference is quite big, cells are detached one by one (Fig. 4b). In the second one, for large forces difference cells are detached individually (Fig. 4c). The boundary between these three models has not been defined till now. Generally, cells do not adhere flat to the substrate, but oscillate between the free state and the bound state. A lack of shear stress causes large energy differences besides those two states. In dynamic conditions the energy level between those two states equalizes and probability of cells detachment from surface is 50%, what is determined by critical stress.

To study detachment kinetics, a radial flow chamber was applied, varying the duration of exposure to shear flow from 10 to 25 minutes. Each material was examined with individu-

al time parameters. The exposure time for each material was regarded individually to enable kinetic calculations.

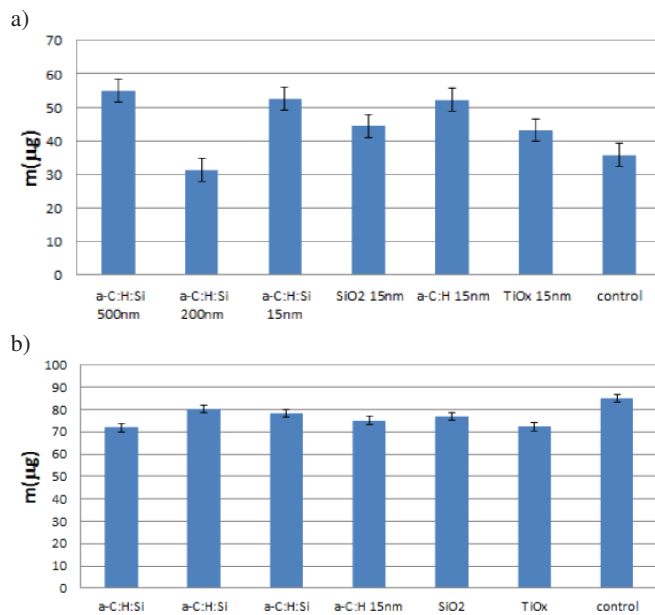


Fig. 4. Protein material interaction: a) based on interaction with FBS solution, b) based on interaction with whole blood

Shear stress. The dependence of detached cells on applied shear stress is the measure of mechanical interaction between cells and substrates. If the applied forces are sufficient, cells are removed from the solid surface and are taken away by the flow. In radial geometry, shear stress decreases with inverse proportion to the distance, r , and to the flow origin according to:

$$\sigma_{50\%} = \frac{3D\eta}{\pi r_{50\%} e^2}, \quad (1)$$

where D is the flow rate, which depends on the material, η is the dynamic viscosity of the fluid (10 g/(cm*s)), and e is the distance between the disk and the plate. For these experiments, e was set at 150 μ m.

Based on the cell detachment from the surface cell detachment rate was calculated. It is defined as a number of detached cells per minute. Detachment rate was calculated for each investigated material in the form of thin film.

3. Results

3.1. Mechanical properties of the coatings. In order to select material with the best cohesion and the lowest friction, the scratch test with Rockwell indenter was performed. It inserts high stress with low loads inside material. SiO₂ reveals the greatest depth of destruction caused by the applied load (Table 1). Reducing the thickness of the coating a-C:H:Si does not result in a proportional reduction in scratch depth. All coatings being in contact with diamond indenter reveal a low friction coefficient.

Table 1

The maximum depth of cracks after unloading h_r , and the friction coefficient at maximum load

Sample	Scratch depth h_r [μm]	Friction coefficient
a-C:H 15 nm	12.2	0.33
a-C:H:Si 15 nm	12.6	0.32
a-C:H:Si 200 nm	12	0.34
a-C:H:Si 500 nm	12.4	0.36
SiO ₂ 15 nm	14.3	0.36
TiO _x 15 nm	12.3	0.37

Resistance to abrasion and wear is an increasingly important property of the surface of modern materials. Specific paints and coatings are frequently developed that require detailed characterization of their scratch resistance. At a given constant load smallest deformation of the a-C:H:Si 500 nm coating is observed, because of the greatest thickness (Table 2). For the group of materials having the same thickness 15 nm achieved the greatest penetration depth for a-C:H:Si film.

Table 2

The summarizes of the total system deformation h_{max} , the remaining depth h_0 , defined Young's modulus under the applied load E_{IT}

Sample	Maximal depth h_{max} [nm]	Remaining depth h_0 [nm]	Young modulus E_{IT} [MPa]
a-C:H 15 nm	57100	13030	340
a-C:H:Si 15 nm	56100	14030	351
a-C:H:Si 200 nm	55880	12050	297
a-C:H:Si 500 nm	46500	9560	271
SiO ₂ 15 nm	59200	13950	365
TiO _x 15 nm	58300	12390	311

3.2. Protein-material interactions. Number of adsorbed protein, normalized to albumin, as a function of the tested surface is shown in Fig. 4. For the analysis the positive control was prepared. For FBS solution, the strongest protein-material interaction is observed for a-C:H:Si 500 nm coating (Fig. 5a). Changing the thickness of a-C:H:Si coating to 200 nm cause a significant decreases in adhesion of albumin. Reducing the thickness of the coating to 15 nm results in a renewed increase in the amount of adsorbed protein. For whole blood the opposite trend is observed (Fig. 5b). Weight of protein deposited on the a-C:H:Si 200 nm surface is greater than for 500 nm and 15 nm.

3.3. Cell-material interaction. Cell-material interaction under hydrodynamic conditions: – finite element simulation. The simulation of cell detachment assay by means of the radial flow chamber is presented in Fig. 6. The cell-material interaction varied depending on the shear stress value and the direction of the velocity vector of the flowing medium. According to the material, cell deformation was examined in three places: at the stagnation point where rectangular velocity flow vectors exist, at the highest shear stress, and at the place where low velocity flow was expected.

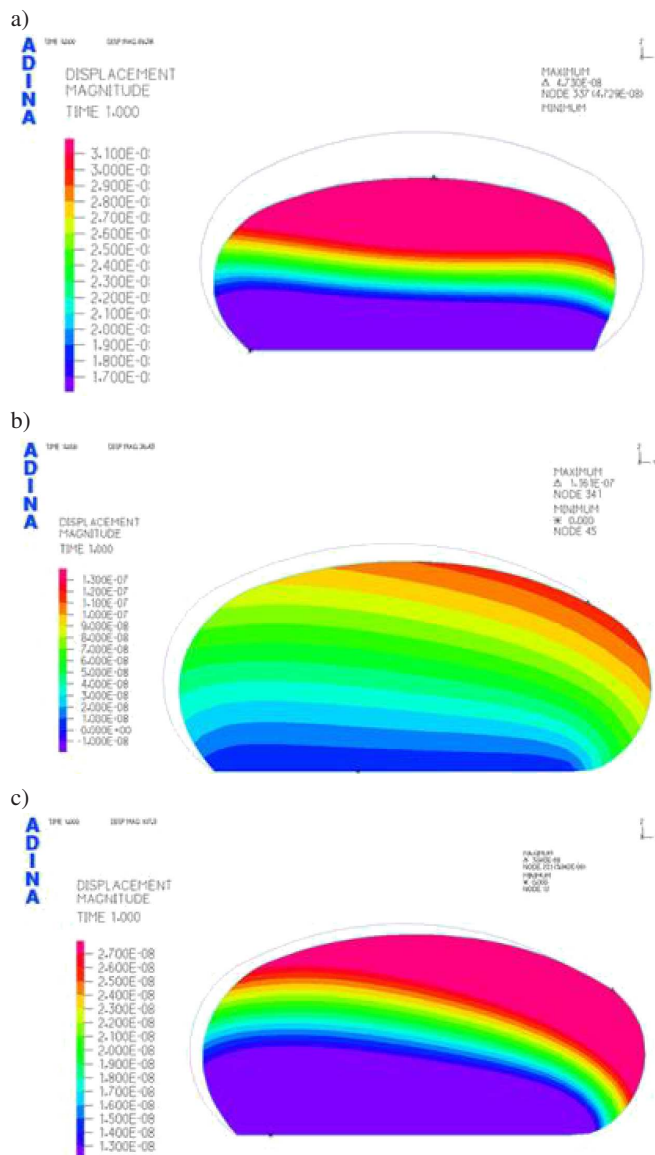


Fig. 5. Finite element modelling of the stress distribution in the cell: a) in the center, b) just behind the hole flow, c) in the outer region of radial flow chamber

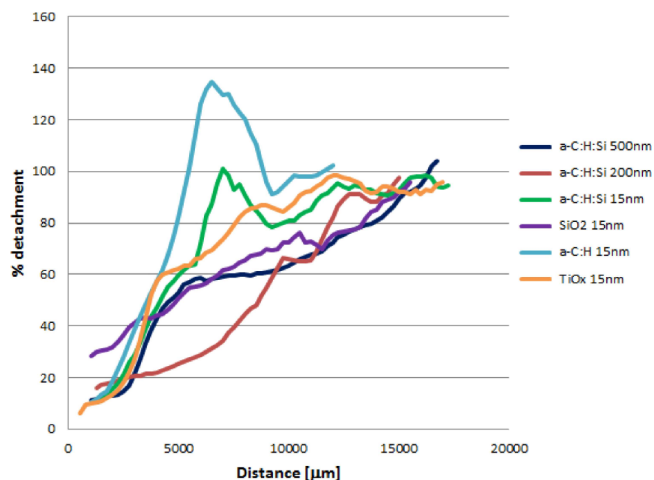


Fig. 6. Detachment kinetics determined as cell adhesion to the substrate in the function of the distance from the center

K. Trembecka-Wojciga, R. Major, J.M. Lackner, F. Bruckert, E. Jasek, and B. Major

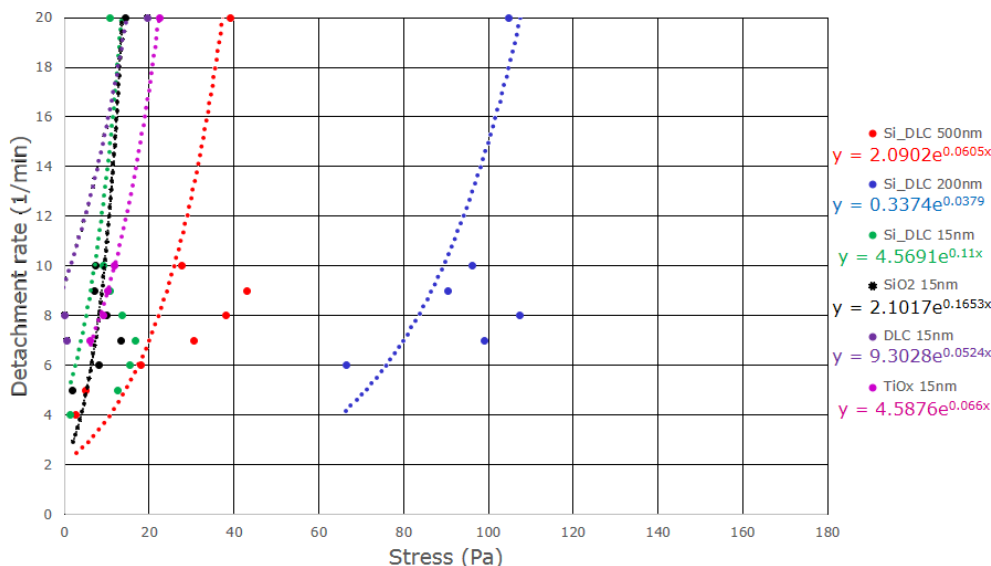


Fig. 7. Detachment rate in function of applied stress

The highest probability of cell detachment was indicated for the location with the highest value of medium velocity, which could cause the highest shear stress. The cell reaction was examined in different locations in the radial flow chamber. In the center, cells were compressed (Fig. 6a). In the location with the highest shear stress, cells were deformed by tensile and compressive stress (Fig. 6b). Similar reactions occurred for the outer region of the central cell position (Fig. 6c).

Cell-material interaction under hydrodynamic conditions: radial detachment test. Cells were deposited with a density of 300 cells/mm² and gently washed with a minimal shear stress. The results provide information about the amount of weakly and strongly bonded cells. Microscopic observations revealed differences in the number of cells depending on the material type. A different cell distribution was observed depending on the material used.

The main criteria for selection of the red blood cells concentrate was the possibility of analysis and visualization of individual cells after shear forces. It was necessary to estimate the shear stress between the individual cell and the surface of the tested sample. 14ml of the solution for each tested coating was used.

Detachment kinetics. Several experiments were performed to study the detachment kinetics. Cell adhesion to the substrate was determined by the percentage of the cells remained in the function of the distance from the center (Fig. 7).

The number of adhered red blood cells on the surface was counted through the radius of the plate starting from the center of the disk. There is no possibility to count adhered cells before fluid flow in radial flow chamber. The number of erythrocytes counted in the edge of the disk is taken as an average number of adhered cells before test – without applying shear stress. At this point the value of applied shear forces is the smallest and there is no detachment of cells from surface.

The diagram presents the valley like cell distribution (Fig. 7). In the initial part of the graph, in the distance close

to the central point the highest shear stress occurs. It causes the greatest cell washout here. With the distance the shear stress is lower. This results in an increase in the number of cells along the radius until reaching a plateau. Diagrams in the shape of wide and deep valleys are characterized by a weak cell- materials interaction. This demonstrates the wide field of the cell detachment under the shear forces introduction. Diagrams in the shape of narrow and shallow valleys, represent materials with strong interaction with cells. In this case, washout is weak. In two cases, the number of counted cells exceeds 100%. This may be the result of cell migration across the surface.

Detachment rate. Based on the results presented in Fig. 7, detachment rate was calculated. Detachment rate shows how fast cells could be removed under a given shear stress (Fig. 8).

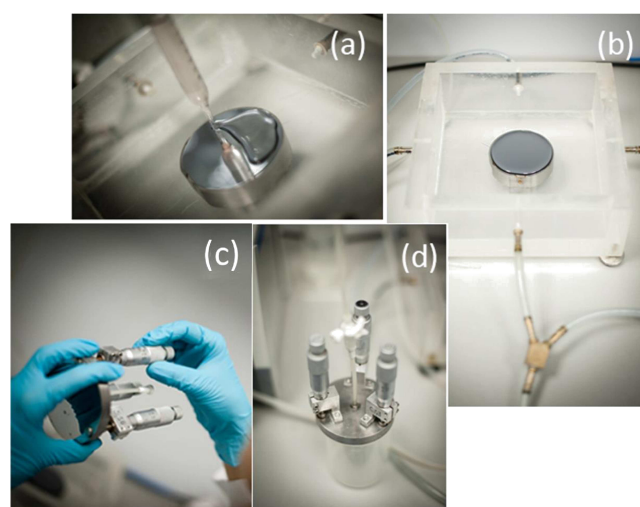


Fig. 8. Stages of the performance analysis using a radial flow chamber: a) cell deposition, b) cell seeding, c) disc adjustment, d) system assembling

Biomechanical properties of the thin PVD coatings defined by red blood cells

The exponential function extrapolation to the shear stress equal zero determines spontaneous rate of the cell detachment. This indicates how fast cells would be removed from the tested surface without applied shear stress induced by flow. Spontaneous velocity values obtained are summarized in Table 3.

Table 3
Spontaneous detachment rate

Sample	Spontaneous detachment [1/min]
a-C:H 15 nm	9.30
a-C:H:Si 15 nm	$8 \cdot 10^{-8}$
a-C:H:Si 200 nm	4.57
a-C:H:Si 500 nm	2.10
SiO ₂ 15 nm thick	2.09
TiO _x 15 nm	4.58

Detachment threshold stress. The efficiency exhibits the stress threshold behavior. For each coating material, a wide range of stress levels was studied in a single experiment (Fig. 9). Tests were planned individually for each material. Values of applied forces were calculated by using Eq. (1). The efficiency of cell detachment from the substrate was presented in Fig. 8. Elution of cells from surface increases with increasing values of applied stress until plateau. After that increasing values of applied forces do not have influence of cells movements. There is no 100% of red blood cells detachment for any tested material.

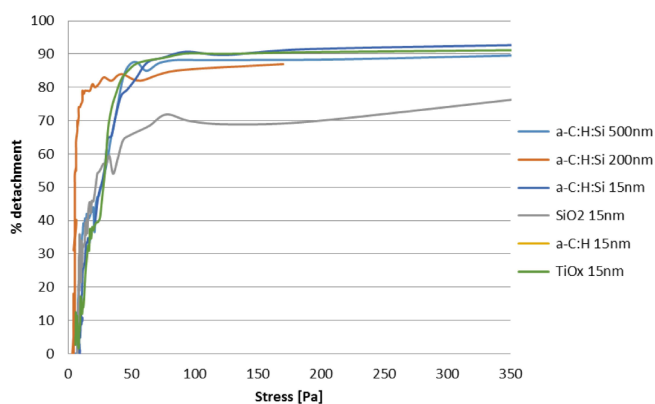


Fig. 9. The efficiency of cell detachment from the substrate

The strongest cell material interaction was observed for SiO₂, although the not the highest values of the threshold stress. Figure 9 indicates exceeding 40 Pa, cells detach with a probability of 80%. The highest values of the applied shear stress were not able to remove all cells from the surface due to strong cell-material interaction. For a-C:H:Si 200 nm, the highest efficiency of cell removal occurred for exceeding 20 Pa. The detachment efficiency function looks different for the case of a-C:H:Si 500 nm where the maximum occurs at higher values of stress. A plateau was observed for the stress value exceeding 8 Pa. For all the samples except SiO₂, cells were removed with efficiency between 90–100% for the highest shear stress. The stress necessary to remove 50% of

the cells is defined as the threshold stress and is labeled as $\tau_{50\%}$. a-C:H:Si 200 nm surfaces exhibit the lowest interaction with the investigated when compared to a-C:H:Si 15 nm and 500 nm (Fig. 10).

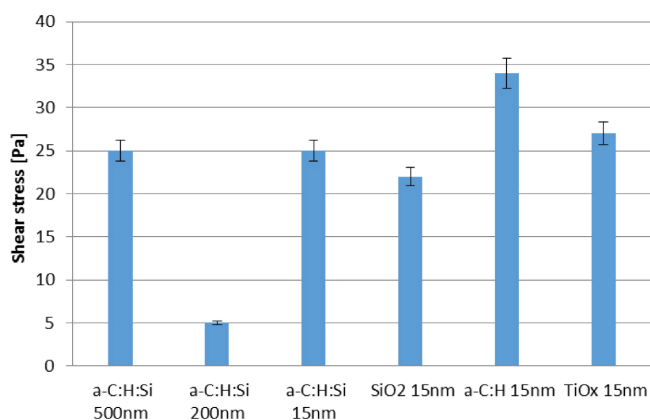


Fig. 10. Threshold stress values

4. Discussion

The paper proposes a new approach to the analysis of properties of biomaterials consisting of bio and haemo tribological test. Test considered the radial flow chamber where the single blood cell was regarded and the cell-material shear stress was the main factor for the material selection. In the modern technology, the surface of a material represents far more than only the delamination of its solid cross section. It is rather the place for all interactions of components with its environment [14]. Surface treatments- physical modification are effectively done by plasma techniques to shape the surface. Formation of this biomimetic nano-topography and surface chemistry is planned to be performed on the whole surface of the polyurethane membrane, which is novelty, thus, it should be subjected to detail research study. It is planned plasma etching in the project, plasma deposition, chemical deposition of organic and inorganic films and plasma grafting with functional molecules (e.g. amine, carboxyl groups), respectively. Both, full chemical/topographical homogeneity and gradients are expected for targeted protein as well as blood elements. The technique under consideration allows preparing the optimal surface charge by the application of hydrophilic or hydrophobic materials.

The combination of the advanced material science and biology is a new future of an advanced concept to design materials for the blood contact. Up to now most of the materials which are used for the heart support system and replacement are based on carbon, titanium or natural tissue prepared from porcine [15–28]. The aim of this study was to study biotribological aspects of the thin coatings, elaborated de novo for the direct blood contact. The work focused on haemocompatible films. Analysis of the mechanical properties was correlated with protein adsorption and mechanical study of the blood-material interaction. Similar aspects were pointed out by the other authors [29]. There is no perfect test that would allow determining explicitly the biomechanical properties. Due to

a high physiological variation in blood morphology, mainly platelet of red blood cells count, credible results can be obtained using 8–10 replicates of the test, as was demonstrated by other authors [30, 31]. Moreover, the tests are also very sensitive to the imperfect smoothness of the surface. This limitation can be evaded using a high quality test plates.

Variations in critical stress of presented materials may be explained due to differences of the contact angle. This effect is particularly interesting for coating of a-C:H:Si. This coating was prepared in three thickness variants. A low value of the threshold stress may indicate hydrophobic properties of the surface of coating. The high value of the stress indicates the hydrophilic properties. Critical stress corresponds to the amount of adsorbed protein in the serum. The results were normalized to the albumin as the most prominent blood protein. The character of the graph was different for the analysis of protein adsorption from whole blood. Coatings which were characterized by low values of the critical shear forces in the interaction with the red blood cells and low serum adsorption of proteins from serum, expressed the increased adsorption of albumin from whole blood. This demonstrates the probability of impact of the additional blood factor affecting the change in the physical properties of the material surface.

5. Conclusions

Developing novel, low thrombogenic materials is of the central importance. The presented work is focused on processing of coating with improved biocompatibility. Within the frame of the work biotribological tools were developed. Based on the results the following conclusions could be formed:

- tribological test results showed high adhesion to the substrate which indicates a properly designed and carried out process of the thin coatings deposition;
- mechanical analyzes did not reveal differences between the a-C:H:Si coatings phase depending on the thickness. Differences were detected in the analysis of protein adsorption and confirmed in the biotribological analysis of the interaction of red blood cells and the test surface. Coating thickness a-C:H:Si intermediate characterized by both reduced interaction with the protein properties as well as from blood cells. This confirms the thesis that the integration of scientific fields is necessary for explanation of all the phenomena occurring at the tissue – material border;
- the strongest cell – material interaction was observed for the carbon-based coatings. A high value of the shear stress in the radial flow chamber did not remove all cells from the surface;
- numerical methods cannot explain all phenomena and predict all reactions, especially with cells. However, they are a valuable tool to assist in planning and verification of the experiment. Finite element methods were used to plan the experiment on the shear forces in the material-cell (red blood cell) interaction.

Acknowledgements. This research was financially supported by the project 2011/03/D/ST8/04103 “Self-assembling, bio-

mimetic porous scaffolds in terms of inhibiting the activation of the coagulation system” of the Polish National Center of Science.

REFERENCES

- [1] R. Kustosz, M. Gawlikowski, K. Gorka, and A. Jaros, “Structure of research stand and evaluation method of blood- biomaterial reaction and mechanical strength of the coating”, in *Nanostructural Materials for Implants and Cardiovascular Biomedical Devices*, M-Studio, Zabrze, 2011.
- [2] R. Major, “Material science in heart disease treatment”, in *Nanostructural Materials for Implants and Cardiovascular Biomedical Devices*, M-Studio, Zabrze, 2011.
- [3] U.T. Seyfert, V. Biehl, and J. Schenk, “In vitro hemocompatibility testing of biomaterials according to the ISO 10993-4”, *Biomol. Eng.* 19 (2), 91–96 (2002).
- [4] M. Dadsetan, H. Mirzadeh, N. Sharifi-Sanjani, and P. Salehian, “In vitro studies of platelet adhesion on laser-treated polyethylene terephthalate surface”, *J. Biomed. Mater. Res.* 54, 540–546 (2001).
- [5] N. Huang, P. Yang, and Y.X. Leng, “Hemocompatibility of titanium oxide films”, *Biomaterials* 24, 2177–2187 (2003).
- [6] M. Mueller, B. Krolitzki, and B. Glasmacher, “Dynamic in vitro hemocompatibility testing – improving the signal to noise ratio”, *Biomed. Tech.* 57, Suppl. 1 (2012).
- [7] M. Otto, C.L. Klein, H. Koehler, M. Wagner, O. Roehrig, and C.J. Kirkpatrick, “Dynamic blood cell contact with biomaterials: validation of a flow chamber system according to international standards”, *J. Mater. Sci. Mater. Med.* 8, 119–129 (1997).
- [8] D. Varon, I. Lashevski, B. Brenner, R. Beyar, N. Lanir, I. Tamarin, and N. Savion, “Cone and plate(let) analyzer: monitoring glycoprotein IIb/IIIa antagonists and von Willebrand and disease replacement therapy by testing platelet deposition under flow conditions”, *Am. Heart J.* 135, 187–193 (1998).
- [9] D.A. Jones, C.W. Smith, and L.V. McIntire, “Methods for in vitro analysis of leukocyte adhesion under flow condition”, in *Weir’s Handbook of Experimental Immunology*, eds. L.A. Herzenberg, D.M. Weir, and C. Blackwell, Blackwell Science, Cambridge, 1996.
- [10] T. Yago, J. Wu, C.D. Wey, A.K. Klopocki, C. Zhu, and R.P. McEver, “Catch bonds govern adhesion through L-selectin at threshold shear”, *J. Cell Biology* 166 (6), 913–923 (2006).
- [11] J.M. Lackner, W. Waldhauser, R. Major, B. Major, and F. Bruckert, “Hemocompatible, pulsed laser deposited coatings on polymers”, *Biomedizinische Technik* 55, 57–64 (2010).
- [12] L. Tobolski and A. Fee, “Macroindentation hardness testing”, *ASM Handbook, Volume 8. Mechanical Testing and Evaluation*, ASM International, Ohio, 2000.
- [13] M. Demilly, Y. Brechet, F. Bruckert, and L. Boulangue, “Kinetics of yeast detachment from controlled stainless steel surfaces”, *Colloids Surf. B* 51, 71–79 (2006).
- [14] R.A. Haefer, *Oberflächen- und Dünnschichttechnologie. Teil I: Beschichten von Oberflächen*. Springer, Berlin, 1987.
- [15] C. Valfrè, G. Rizzoli, C. Zussa, P. Ius, E. Polesel, S. Mirone, T. Bottio, and G. Gerosa, “Clinical results of Hancock II versus Hancock Standard at long-term follow-up”, *J. Thorac Cardiovasc Surg.* 132, 595–601 (2006).
- [16] M.A. Borger, J. Ivanov, S. Armstrong, D. Christie-Hrybinsky, C.M. Feindel, and T.E. David, “Twenty-year results of the Hancock II bioprosthesis”, *J Heart Valve Dis.* 15, 49–56 (2006).

Biomechanical properties of the thin PVD coatings defined by red blood cells

- [17] P. Totaro, N. Degno, A. Zaidi, A. Youhana, and V. Argano, "Carpentier-Edwards PERIMOUNT Magna bioprosthesis: a stented valve with stentless performance?", *J. Thorac Cardiovasc Surg.* 130, 1668–74 (2005).
- [18] F.C. Riess, R. Bader, E. Cramer, L. Hansen, B. Kleijnen, G. Wahl, J. Wallrath, S. Winkel, and N. Bleese, "Hemodynamic performance of the medtronic mosaic porcine bioprosthesis up to ten years", *Ann. Thorac Surg.* 83, 1310–89 (2007).
- [19] G. Cohen, G.T. Christakis, C.D. Joyner, C.D. Morgan, M. Tamariz, N. Hanayama, H. Mallidi, J.P. Szalai, M. Katic, V. Rao, S.E. Fremes, and B.S. Goldman, "Are stentless valves hemodynamically superior to stented valves? A prospective randomized trial", *Ann. Thorac Surg.* 73, 767–78 (2002).
- [20] M.A. Borger, K. Prasongsukarn, S. Armstrong, C.M. Feindel, and T.E. David, "Stentless aortic valve reoperations: a surgical challenge", *Ann. Thorac Surg.* 84, 737–44 (2007).
- [21] S. Lopez, P. Mathieu, P. Pibarot, S. Mohammadi, F. Dagenais, P. Voisine, J. Dumesnil, and D. Doyle, "Does the use of stentless aortic valves in a subcoronary position prevent patient-prosthesis-mismatch for small aortic annulus?" *J. Card. Surg.* 23, 331–5 (2008).
- [22] D.S. Bach, N.D. Kon, J.G. Dumesnil, C.F. Sintek, and D.B. Doty, "Ten-year outcome after aortic valve replacement with the freestyle stentless bioprosthesis", *Ann. Thorac Surg.* 80, 480–7 (2005).
- [23] R.W. Emery, C.C. Krogh, K.V. Arom, A.M. Emery, K. Benyo-Albrecht, L.D. Joyce, and D.M. Nicoloff, "The St. Jude Medical cardiac valve prosthesis: a 25-year experience with single valve replacement", *Ann. Thorac Surg.* 79, 776–82 (2005).
- [24] R. Tominaga, K. Kurisu, Y. Ochiai, Y. Tomita, M. Masuda, S. Morita, and H. Yasui, "A 10-year experience with the CarboMedics cardiac prosthesis", *Ann Thorac Surg.* 68, 784–9 (2005).
- [25] J. Aagaard and J. Tingleff, "Fifteen years' clinical experience with the CarboMedics prosthetic heart valve", *J. Heart Valve Dis.* 14, 82–8 (2005).
- [26] T. Takaseya, T. Kawara, S. Tokunaga, M. Kohno, Y. Oishi, and S. Morita, "Aortic valve replacement with 17-mm St. Jude Medical prostheses for a small aortic root in elderly patients", *Ann. Thorac Surg.* 83, 2050–3 (2007).
- [27] C. Stefanidis, A.M. Nana, D.D. Cannie're, M. Antoine, J.-L. Jansens, C.-H. Huynh, and J.-L. Le Clerc, "10-year experience with the ATS mechanical valve in the mitral position", *Ann. Thorac Surg.* 79, 1934–8 (2005).
- [28] T. Bottio, L. Caprili, D. Casarotto, and G. Gerosa, "Small aortic annulus: the hydrodynamic performances of five commercially available bileaflet mechanical valves", *J. Thorac Cardiovasc. Surg.* 128, 457–62 (2004).
- [29] A. Qiao and Y. Liu, "Medical-application-oriented hemodynamics simulation (I): blood flows in arteries", *J. Beijing University of Technology* 02, CD-ROM (2008).
- [30] http://www.bdbiosciences.com/external_files/pm/doc/tds/human/live/web_enabled/31255X_555483.pdf.
- [31] http://www.bdbiosciences.com/external_files/pm/doc/tds/human/live/web_enabled/31794X_555523.pdf.